CHARACTERIZATION OF SILICON/GLASS ANODIC BOND INITIATION TOUGHNESS

Paul E. W. Labossiere, Martin L. Dunn, and Shawn J. Cunningham*
Department of Mechanical Engineering, University of Colorado, Boulder, Colorado
*Microcosm Technologies, Inc., Colorado Springs, Colorado

ABSTRACT

We describe an approach to characterize the initiation toughness (resistance of anodic bonded interfaces to crack initiation) of silicon/glass anodic bonds. The approach is based on the existence of a universal stress state at the most common site of fracture initiation, the silicon/glass interface corner. In order to validate the approach we designed and fabricated relatively simple anodic bond test specimens and carried out a mechanical test program to characterize the initiation toughness. We find that while failure stresses vary significantly with bond area, the initiation toughness is independent of bond area.

INTRODUCTION

Anodic bonding has become a common process in the wafer-level packaging of microelectromechanical systems (MEMS). It has been used in the manufacturing of accelerometers [1,2], pressure sensors [2], micropumps [3], tactile sensors [4], and flow sensors [5]. In any product manufactured using anodic bonding, a fundamental understanding of bond failure mechanisms can be used in the design process to improve robustness and reliability. For example, Figure 1 shows an early prototype accelerometer that has been mounted to a copper lead frame (manufactured and donated by Ford Microelectronics, Inc.). The prototype demonstrates the technology for a silicon accelerometer anodically bonded to glass with an anodically bonded silicon lid to encapsulate the accelerometer. The technology was used in future products.

The many practical applications of anodic bonding have generated substantial interest in the mechanical integrity of silicon/glass anodic bonds. While often bond quality, although a nebulous concept, is established by qualitative visual inspection (for example, optical, infrared, and acoustic microscopy), the mechanical integrity has been established empirically through tensile or shear testing of bonded dies [6-9], but is not well understood fundamentally. In fact, the information obtained from such tests (typically the failure load) is not broadly applicable as it depends on the specimen size, geometry, and the type of loading. This is due to the complexity of the stress state at the interface corner which drives failure and rendered the use of a strength-based failure criterion inappropriate.

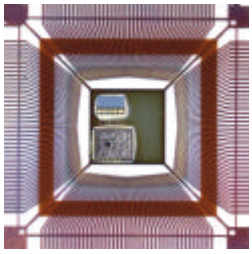

Figure 1. Accelerometer prototype by Ford Microelectronics Inc. showing microelectronic circuit and silicon/glass encapsulated proofmass.

Alternatively, Hurd et al. [10] and Go and Cho [11] have attempted to correlate fracture of silicon/glass anodic bonds by applying the concepts of elastic interface fracture mechanics. Interface fracture mechanics (see Rice, [12] and Hutchinson and Suo, [13] for detailed discussions) seems to be a more appropriate framework within which to interpret the mechanical integrity of anodic bonds than tensile, shear, or burst strength because the results may be independent of specimen size and geometry. Nevertheless, its applicability to silicon/glass anodic bonds is problematic, and not strictly valid. This is because fracture typically initiates at a discontinuity (the silicon/glass interface corner) where no preexisting cracks are observed; such preexisting cracks are required for the application of fracture mechanics. An additional requirement is that the crack must run along the interface; however, when fracture occurs in silicon/glass anodic bonds, usually the crack *does not* propagate along the tough interface, rather it dives into the glass. Finally, both Tatic-Lucic et al. [9] and Go and Cho [11] have studied the effects of various processing

parameters, for example bonding voltage and temperature, on the mechanical integrity of silicon/glass anodic bonds. Our proposed approach can also be used to study the effects of processing parameters on mechanical integrity, but as we will argue, it can be more broadly applied.

Our primary goal is to provide a rigorous mechanics-based framework to assess the *initiation toughness* of anodic bonds that can be used both to rank bond toughness as a function of processing parameters and to facilitate the design of reliable bonds. In this paper we describe the development and application of this framework. It is based on correlating fracture initiation at the silicon/glass interface corner with a critical value of the stress intensity that results from a linear elastic stress analysis. It is in the spirit of interface fracture mechanics, but overcomes the two obstacles described above. We are motivated by recent success using this type of approach by Reedy and Guess [14-16] for adhesively-bonded butt joints and Dunn et al. [17] and Suwito et al. [18] for homogeneous notches in acrylic and silicon, respectively. The framework is intended to be universal in that it is independent of the bond size (area). As such, it can be applied to rank bond toughness as a function of processing parameters (and thus discriminate between different failure modes) to facilitate the design of reliable bonds. We describe the design and fabrication of the anodic bond test specimens and discuss the mechanical test program. Then we discuss the nature of the stress state at the silicon/glass interface corner and its implications for failure analysis. We then apply the fracture initiation criterion to the measurements and discuss the results.

SPECIMEN FABRICATION AND MECHANICAL TESTING

Silicon/glass anodic bond specimens were fabricated from four inch (100) silicon and BOROFLOAT™ borosilicate glass wafers. The silicon wafers were 380 μm thick, double side polished, n- silicon with a resistivity of 10^{-2} Ω-cm and cubic elastic constants (in the natural crystal system) of C_{11} = 165.7 GPa, C_{12} = 63.9 GPa, and C_{44} = 79.6 GPa [18]. The glass wafers were 580 μm thick, and assumed isotropic with Young's modulus and Poisson's ratio of E = 63.0 GPa and ν = 0.2, respectively.

Two etch processes were used: wet chemical etching in KOH or deep reactive ion etching (DRIE) to create trenches in the silicon wafer. The etched silicon wafer was then anodic bonded to the glass wafer to reveal interface corners with 54.7° or 90° interface corners, for the wet or DRIE etched silicon wafers, respectively. The bonded wafers were then diced to produce test dies (2w = t = 3 mm) consist of anodic bonded regions (h = 100 μm) that traverse the full length of the die, but have bond lengths of 2a = 200, 400, 700, 1000, and 1400 microns. A scanning electron micrograph of a typical specimen is shown in Fig. 2; complete fabrication details are given elsewhere [19].

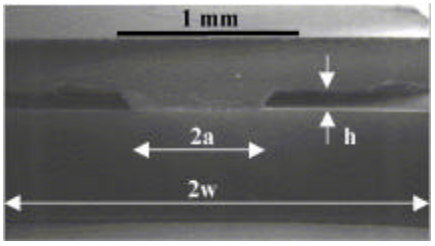

Figure 2. Scanning electron micrograph of a typical silicon/glass anodic bond specimen.

The silicon/glass specimens were bonded to aluminum studs about 25 mm long with a 3mm x 3mm square cross section. The effect of elastic mismatch between the studs and the specimen was considered in the data reduction and found to be insignificant. The specimens were then loaded in the offset three-point flexure configuration shown in Fig. 3. The load offset distance, *l*, can be chosen to vary the relative shear force and bending moment at the interface corner, and thus the mode mixity (loosely, shearing vs. opening) at the interface corner. In our tests, we used *L* = 35 mm and *l* = 2.5 mm. The specimens were loaded in a servo-hydraulic mechanical test frame under load-point displacement control at 0.01 mm/sec.

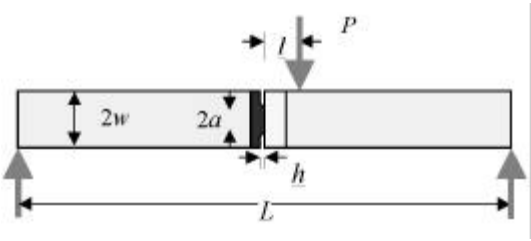

Figure 3. Schematic of offset three-point flexure test setup. The specimen depth is $t = 2w$.

In all cases, the load-displacement response was linear until brittle fracture which consisted of a crack that initiated at the silicon/glass interface corner on the tensile side (bottom) of the specimen. The crack did not necessarily propagate along the interface. For some specimens, the crack dove into the glass at an angle of about 45 degrees from the interface, and then turned and ran through the glass resulting in ultimate failure. A

photograph of representative failed specimens are shown in Fig. 4.

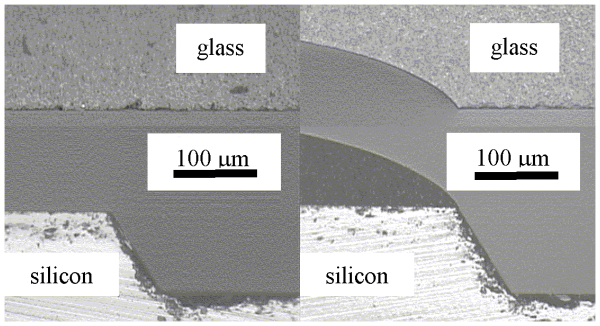

Figure 4. Photograph of failed specimens with *weak* interfaces and *strong* interfaces.

STRESS AND FAILURE ANALYSIS

The interface corner of the silicon/glass anodic bond can be described by a glass half-plane bonded to a silicon plane with an opening angle γ. Near the interface corner (asymptotically) the in-plane stress and displacement fields can be expressed as:

$$\begin{aligned} s_{ij}^{M} &= K_1^n r^{l_1-1} f_{ij}^{1M}(q) + K_2^n r^{l_2-1} f_{ij}^{2M}(q) \\ u_i^{M} &= K_1^n r^{l_1} g_i^{1M}(q) + K_2^n r^{l_2} g_i^{2M}(q) \end{aligned} \qquad (1)$$

Here K_m^n (m = *1, 2*) are stress intensities, λ-1 are the strength of the stress singularities, and f_{ij}^m and g_i^m (m = *1, 2*) are functions which depend on q and differ for each material (M = *A, B*). The sub and superscripts *1,2* denote deformation modes that are analogous to the opening and sliding modes in a homogeneous solid with a notch of opening γ; however, they are not in general symmetric and antisymmetric with respect to the notch bisector. Although not explicitly noted, K^n, l-1, f_{ij} and g_i are functions of the anisotropic elastic stiffnesses of both materials, and when in-plane and antiplane deformations are decoupled, they depend on whether plane strain or plane stress conditions prevail. In eq. (1) l, f_{ij}, and g_i can be determined from an asymptotic analysis of the stress state near the interface corner (see for example, Ting [20]). Only the stress intensities K_1^n and K_2^n can not be determined from the asymptotic analysis. They depend on the far-field loading and geometry of the solid.

We computed the orders of the mode 1 and 2 singularities from the asymptotic analysis described briefly above (details can be found elsewhere [21]) and found for the silicon/glass interface corner with γ = 54.7° that the stress singularities are λ_1-1 = -0.497 and λ_2-1 = -0.364 and with γ = 90° that the stress singularities are λ_1-1 = -0.494 and λ_2-1 = -0.188. Interestingly, for both γ = 54.7° and γ = 90°, λ_1-1 are nearly as strong as that for a crack (-0.5), while λ_2-1 are smaller, although not obviously insignificant.

Dimensional considerations dictate that the stress intensities for the specimen, material combination, and loading shown in Figs. 2 and 3 can be written in the form:

$$K_i^n = s^o w^{1-l_i} Y_i\left(\frac{a}{w}\right) \quad (i=1,2) \qquad (2)$$

The nominal stress is defined as the normal stress that would exist at the surface of a homogeneous beam of height *2w* and depth *t* (= *2w*) under the three-point flexure loading, i.e.,

$$s^o = \frac{3M}{2tw^2} = \frac{3P(L/4 - l/2)}{4w^3} \qquad (3)$$

We carried out finite element calculations to determine Y_1 and Y_2 as a function of *a/w*. Y_1 and Y_2 were obtained from the finite element solution in two ways: matching the finite element solution near the interface corner with the asymptotic displacements of eq. (1), and through use of a path-independent contour integral. Both techniques are described in detail elsewhere [21].

In as much as the stress field near the interface corner of the silicon/glass anodic bond (where fracture initiates) is described by K_1^n and K_2^n, it is reasonable to pursue the development of a criterion for fracture initiation based on some combination of K_1^n and K_2^n. Specifically, in the spirit of Irwin for classical fracture mechanics, we postulate a fracture initiation criterion as $f(K_1^n, K_2^n) = f_c$. Put simply, this says that fracture will initiate at the interface corner when some combination of K_1^n and K_2^n reaches a critical value f_c. The criterion only addresses initiation; the subsequent propagation is a related, but different problem. In general, the functional form of $f(K_1^n, K_2^n)$ and the critical value must be determined experimentally. See Dunn et al. [19] for a complete discussion.

The argument for the possible success of this fracture criterion parallels that for the fracture mechanics of interface cracks (see Rice [12] for a discussion). We know that the asymptotic solution is not a good approximation very close to the interface corner (it is

perturbed by material nonlinearities or small-scale heterogeneities and irregularities) nor is it a good approximation very far from the interface corner (it is perturbed by the finite geometry). The solution is thus only a good approximation for the elastic fields in an annulus surrounding the interface corner; the K-annulus. Thus, the magnitudes of K_1^n and K_2^n provide boundary conditions for the region where fracture initiates. Details that do not affect K_1^n and K_2^n do not affect the near-tip fields. If these conditions hold, it should be possible to correlate fracture initiation with critical values of K_1^n and K_2^n. However, such a failure criterion is valid only for a particular interface corner angle because the structure of the asymptotic fields depends on the angle.

The ideas here are obviously generalizations of those of fracture mechanics of brittle interface cracks where fracture is correlated with critical values of the stress intensity factors. As in interface fracture mechanics, the underlying idea here is that of K dominance. An important difference is that with interface cracks, an alternate formulation based on energy considerations agrees with the stress intensity formulation. Such a connection with energetic arguments is lacking with the proposed fracture criterion. As such, it is really only valid for fracture initiation. We contend that a criterion applicable only to fracture initiation is quite valuable, though, particularly for brittle interface corners. Once fracture initiates at the interface corner, a crack will grow in either an unstable or a stable manner. If the former is the case, the situation is catastrophic and the entire problem is described by initiation alone. If the latter is the case, after initiation one can turn to either classical or interface fracture mechanics (depending on whether the crack propagates into one of the adherends or along the interface) to treat the problem of stable crack growth. Finally, given the general mixed-mode fracture initiation criterion $f(K_1^n, K_2^n) = f_c$, there may be situations where simplifications can be made. One such case is when the strength of the mode 2 stress singularity is small compared to that for mode 1. The suitability of such a postulate can only be validated experimentally and this will be discussed in detail in the next section for the silicon/glass anodic bonds considered here.

APPLICATION OF THE PROPOSED FRACTURE INITIATION CRITERION

If fracture initiation can be correlated with critical stress intensities, then we can use the specimen dimensions along with the measured failure stress in eq. (3) to compute critical values of K_1^n and K_2^n. If the K_1^n and K_2^n so obtained do not vary with changes in geometry (bond length *a/w* in the present case), this suggests that they can be used in a universal manner to correlate fracture initiation. Given the dominance of the mode 1 stress singularity, we will attempt to correlate fracture initiation based only on a critical value of K_1^n. Our thinking is based on previous success in mixed-mode loading of 90° corners in homogeneous acrylic [17] and silicon [18], although in those studies the strength of the mode 2 singularity was weaker than it is here. Two sets of anodic bond specimens with $\gamma = 54.7°$ were fabricated in different batches and will be referred to as set A and B. The results suggests that critical $K_{1cr}^n = 0.24$ MPa $m^{0.497}$ and $K_{1cr}^n = 0.09$ MPa $m^{0.497}$ can be used to correlate fracture initiation from the $\gamma = 54.7°$ silicon/glass interface corner for specimens from sets A and B, respectively. For $\gamma = 90°$ silicon/glass interface corner, the results suggests critical $K_{1cr}^n = 0.19$ MPa $m^{0.494}$. This can be seen in Figs. 5 and 6 where the measured failure stresses are plotted as a function of *a/w* for $\gamma = 54.7°$ and $\gamma = 90°$, respectively. Also shown are the predicted failure stresses based on the critical stress intensity failure criterion (with $K_{1cr}^n = 0.24$ MPa $m^{0.497}$ for set A and $K_{1cr}^n = 0.09$ MPa $m^{0.497}$ for set B for $\gamma = 54.7°$ and $K_{1cr}^n = 0.19$ MPa $m^{0.494}$ for $\gamma = 90°$), i.e.,

$$\sigma_{cr}^{o} = \frac{K_{1cr}^n w^{\lambda_1 - 1}}{Y_1\left(\frac{a}{w}\right)} \qquad (4)$$

The observed dependence of failure stress on bond area (which undermines any nominal strength approach to fracture correlation) is well-described by the critical stress intensity failure criterion. Although the results suggest that we can successfully correlate fracture initiation with only the critical mode 1 stress intensity, we do not claim to have fully answered the question of the effects of mode mixity. Studies to completely address mixity effects are underway and the results will be presented elsewhere.

An interesting and important aspect of the proposed failure criterion is the ability to distinguish different failure modes, for the same interface corner geometry, via the measured K_{1cr}^n. To understand this, recall that for 54.7° specimens of set A, the $K_{1cr}^n = 0.24$ MPa $m^{0.497}$ obtained from the tests described in this work

corresponds to a fracture mode of a crack that initiates at the interface corner and propagates into the glass. The strength of the interface was much weaker for set of silicon/glass specimens from set B. In these tests, the fracture mode was a crack that again initiated at the interface corner, but propagated along the interface. In this case, we obtained a K_{1cr}^{n} that was about 0.09 MPa $m^{0.497}$; substantially less than 0.24 MPa $m^{0.497}$. In both cases a crack initiated at the interface corner, but the angle of the initial crack extension differed (thus a different failure mode), as did the subsequent crack propagation path. Of course, our proposed approach is only applicable to the initiation process. The approach can also be used to predict fracture initiation under different far-field loadings (for example tension) due to the universal nature of the stress state at the interface corner.

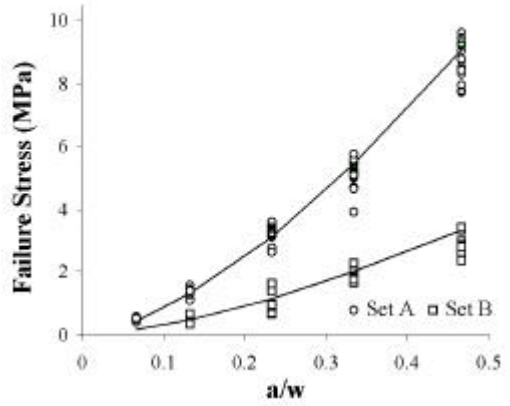

Figure 5. Failure stress vs. bond area for the $\gamma = 54.7°$ specimens. Symbols are measurements and lines are predictions based on the fracture initiation criterion.

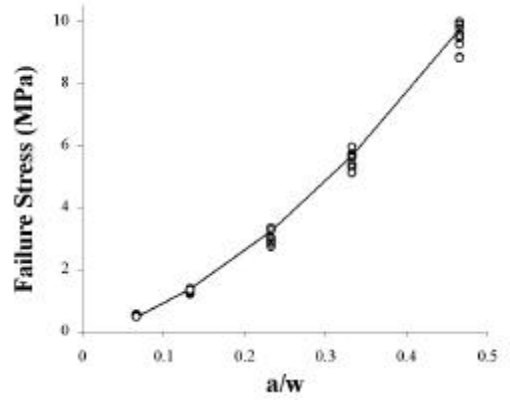

Figure 6. Failure stress vs. bond area for the $\gamma = 90°$ specimens. Circles are measurements and the line is a prediction based on the fracture initiation criterion.

Finally, we comment on the practical application of the proposed approach to the design of anodic bonds. It can be used to characterize the effects of processing parameters on interface toughness in the same manner that tension, shear, and blade tests are currently used (see for example, [9]). In the tension and shear tests, apparent strength results are only applicable for that particular load type, geometry, and failure mode. They can be used to rank bond strengths resulting from different processes, but can be used no further in a quantitative way. Of course, even for use in ranking, there is an implicit assumption that the actual load and failure modes in practice will be the same, or at least similar to these. The present approach is more generally applicable, though. The resulting K_{1cr}^{n} can be used for other load and geometry configurations (that have the same local geometry, i.e., the 54.7° interface corner), because of the universal nature of the stress field at the interface corner. Thus, the K_{1cr}^{n} criterion can be used in conjunction with a stress analysis to design bonded devices. In the application, though, one must be careful to ensure that the failure mode is the same in characterization as it is in practice; for example, crack initiation into the glass versus along the interface. However, one can design the characterization test so that this is the case.

CONCLUSIONS

We described a reasonably simple approach to characterize the initiation toughness of silicon/glass anodic bonded interfaces. The test and the interpretation of the data are based on a rigorous analysis of the stress state at an interface corner where fracture initiates. Unlike interface fracture mechanics of cracks, the approach is applicable to the (common) situations where an initial crack does not exist, and where upon fracture initiation, the resulting crack does not propagate along the interface, but into one of the adherends. The approach was applied to silicon/glass anodic bonded interfaces with 54.7° and 90° interface corners that arises due common etching processes of single crystal silicon. Fracture initiation was accurately correlated with a critical stress intensity of K_{1cr}^{n} = 0.24 MPa $m^{0.497}$ and K_{1cr}^{n} = 0.19 MPa $m^{0.494}$ independent of the bond size for 54.7° specimens of set A and the 90° specimens, respectively. Finally, we discussed how the proposed approach can be used in a quantitative manner in practice to both assess the effects of processing on bond strength, and to design reliable anodic bonds.

REFERENCES

1. Spangler, L. J., and Kemp, C., 1995, "ISAAC-Integrated Silicon Automotive Accelerometer," in *Transducers '95, Eurosensors IX*, Stockholm, Sweden, Vol. 2, pp. 585-588. Also *Sensors and Actuators A*, Vol. 54, pp. 523-529.
2. Esashi, M., Ura, N., and Matsumoto, Y., 1992, "Anodic Bonding for Integrated Capacitive Sensors," MEMS 1992, Proc. IEEE Fifth Ann. Intl. Workshop Micro Electro Mechanical Systems, Travemunde, Germany, pp. 43-48.
3. Acero, M., Plaza, J., Esteve, J., Carmona, M., Marco, S., and Samatier, J., 1997, "Design of a Modular Micropump Based on Anodic Bonding," J. Micromech. Microeng., Vol. 7, pp. 179-182.
4. Chu, Z., Sarro, P., and Middelhoek, S., 1995, "Silicon Three-Axial Tactile Sensor," Transducers '95, Eurosensors IX, 6th Intl. Conf. Solid-State Sensors and Actuators, Stockholm, Sweden, pp. 656-659.
5. Trautweiler, S. F., Paul, O., Stahl, J. and Baltes, H., 1996, "Anodically Bonded Silicon Membranes for Sealed and Flush Mounted Microsensors," MEMS 1996, Proc. IEEE Ninth Ann. Intl. Workshop Micro Electro Mechanical Systems, San Diego, CA, USA, pp. 61-66.
6. Nese, M., and Hanneborg, A., 1993, *Sensors and Actuators*, Vol. A37-38, pp. 61.
7. Obermeier, E., 1995, "Anodic Wafer Bonding," in *Proc. 3rd International Symposium on Semiconductor Wafer Bonding: Physics and Applications*, Electrochemical Society, Vol. 95-7, pp. 212-220.
8. de Reus, R. and Lindahl, M., 1997, in Transducers 97, Proc. of the 9th International Conference on Solid-State Sensors and Actuators, pp. 661-664.
9. Tatic-Lucic, S., Ames, J., Boardman, B., McIntyre, D., Jaramillo, P., Starr, L., and Lim, M., 1997, "Bond Quality Characterization of Silicon-Glass Anodic Bonding," *Sensors and Actuators A*, Vol. 60, pp. 223-527.
10. Hurd, D. S., Caretta, R., and Gerberich, W. W., 1995, "An Experimental Fracture Mechanics Study of a Strong Interface: the Silicon/Glass Anodic Bond," *J. Mater. Res.*, Vol. 10, pp. 387-400.
11. Go, S. J. and Cho, Y.-H., 1998, "Experimental Evaluation of Anodic Bonding Process Using Taguchi Method for Maximum Interfacial Fracture Toughness," in Proc. IEEE Workshop on Microelectromechanical Systems, pp. 318-321.
12. Rice, J. R., 1988, "Elastic Fracture Mechanics Concepts for Interfacial Cracks," J. Appl. Mech., Vol. 55, pp. 98-103.
13. Hutchinson, J. W. and Suo, Z., "Mixed-Mode Cracking in Layered Materials," in *Advances in Applied Mechanics*, Vol. 29, pp. 63-191.
14. Reedy, Jr., E. D. and Guess, T. R., 1993, "Comparison of Butt Tensile Strength Data With Interface Corner Stress Intensity Factor Prediction," *Int. J. Solids Structures*, Vol. 30, pp. 2929-2936.
15. Reedy, Jr., E. D. and Guess, T. R., 1995, "Butt Tensile Joint Strength: Interface Corner Stress Intensity Factor Prediction," *J. Adhesion Sci. Technol.*, Vol. 9, pp. 237-251.
16. Reedy, Jr., E. D. and Guess, T. R., 1998, "Interface Corner failure Analysis of Joint Strength: Effect of Adherend Stiffness," *Int. J. Fracture*, Vol. 4, pp. 305-314.
17. Dunn, M. L., Suwito, W., and Cunningham, S. J., 1997, "Fracture Initiation at Sharp Notches Under Mode I, Mode II, and Mild Mixed-Mode Loading," *International Journal of Fracture*, Vol. 84, pp. 367-381.
18. Mason, W., 1958, *Physical Acoustics and Properties of Solids*, Van Nostrand.
18. Suwito, W., Dunn, M. L., Cunningham, S. J., and Read, D. T., 1999, "Elastic Moduli, Strength, and Fracture Initiation at Sharp Notches in Etched Single Crystal Silicon Microstructures," *Journal of Applied Physics*, Vol. 85, pp. 3519-3534.
19. Dunn, M. L., Labossiere, P. E. W., and Cunningham, S. J., "Initiation Toughness of Silicon/Glass Anodic Bonds," *Acta Materialia*, in press.
20. Ting, T. C. T., 1996, *Anisotropic Elasticity: Theory and Applications*, Oxford Science Publications.
21. Labossiere, P. E. W. and Dunn, M. L., 1999, "Stress Intensities at Interface Corners in Anisotropic Bimaterials," *Engineering Fracture Mechanics*, Vol. 62, pp. 555-575.